

## ARTICLE

# Rigidity of plasticizers and their miscibility in silica-filled polybutadiene rubber by broadband dielectric spectroscopy

Niclas Lindemann<sup>1,2</sup>  | Sebastian Finger<sup>2</sup> | Hossein Ali Karimi-Varzaneh<sup>2</sup>  | Jorge Lacayo-Pineda<sup>2,3</sup>

<sup>1</sup>Institut für Physikalische Chemie und Elektrochemie, Leibniz Universität Hannover, Hannover, Germany

<sup>2</sup>Department of Research and Development, Continental Reifen Deutschland GmbH, Hannover, Germany

<sup>3</sup>Institut für Anorganische Chemie, Leibniz Universität Hannover, Hannover, Germany

## Correspondence

Niclas Lindemann, Institut für Physikalische Chemie und Elektrochemie, Leibniz Universität Hannover, Callinstrasse 3A, Hannover, 30167, Germany.  
Email: niclas.lindemann@pci.uni-hannover.de

## Funding information

This research was funded by the European Union's Horizon 2020 research and innovation program project VIMMP, grant agreement number 760907.

## Abstract

An efficient use of plasticizers in rubber compounds requires an understanding of their miscibility behavior. Besides the chemical properties of both rubber and plasticizer, the rigidity of the plasticizer plays an important role for their miscibility. The miscibility is investigated here using the glass transition measured by differential scanning calorimetry and broadband dielectric spectroscopy (BDS). Additionally, the interfacial relaxation and phase separation measured by BDS are confirmed by transmission electron microscopy. While the flexible plasticizer, poly-( $\alpha$ -methylstyrene), stays miscible in a silica-filled polybutadiene rubber compound, the more rigid plasticizer, indene-coumarone (IC), shows a phase separation at high concentrations. The phase-separated IC tends to accumulate at the silica surface.

## KEYWORDS

dielectric properties, glass Transition, plasticizer, resins, rubber

## 1 | INTRODUCTION

Elastomers are known as a class of versatile materials. The possibility of tuning their properties to meet the requirements for specific applications has made them an important raw material for industrial product. One common way to tune the properties of elastomers is to develop a compound composed of miscible components, as typically practiced for polymer blends in general-purpose elastomers.<sup>1,2</sup> In the case of polymers with a short chain length, or rather oligomers as miscible components, the compound mostly becomes softer, and therefore, these oligomers are called “softeners” or plasticizers. Oils, resins, and

liquid polymers are examples for this category of materials frequently used in tires compounds to optimize their processing and final product performance.

Specifically, blending a plasticizer with a polymer is often required in the rubber industry to achieve the necessary stiffness, good filler dispersion, and enhanced adhesion quality, often associated with a shift in the glass transition temperature, and therefore, with the final characteristics of the product.<sup>3,4</sup> The efficiency of these tuning effects depends on the miscibility between plasticizer and polymer.

In general, a system is miscible if upon mixing  $\Delta G_{\text{mix}} < 0$  and  $\partial^2 \Delta G_{\text{mix}} / \partial^2 \varphi_i > 0$ , where  $\varphi_i$  is the volume fraction of plasticizer,  $\Delta G_{\text{mix}}$  is the free energy of mixing

This is an open access article under the terms of the Creative Commons Attribution License, which permits use, distribution and reproduction in any medium, provided the original work is properly cited.

© 2022 The Authors. *Journal of Applied Polymer Science* published by Wiley Periodicals LLC.

defined as  $\Delta G_{\text{mix}} = \Delta H_{\text{mix}} - T\Delta S_{\text{mix}}$  with the mixing enthalpy  $\Delta H_{\text{mix}}$ , the mixing entropy  $\Delta S_{\text{mix}}$  and the temperature  $T$ .<sup>5,6</sup> The entropy contribution  $\Delta S_{\text{mix}}$  decreases with increasing degree of polymerization, therefore the enthalpy contribution  $\Delta H_{\text{mix}}$  dominates the free energy of mixing of polymer blends bearing high molecular weights.<sup>6</sup>

Plasticizers, however, are small molecules compared to the polymer matrix. Hence, the entropic contribution to the miscibility is expected to be essential for the investigation of the miscibility of low molecular weight plasticizers in polymers. The term rigidity refers to the flexibility of a molecule.<sup>7</sup> The rigidity of the small molecules might affect their miscibility, independently of the mechanical softening effect on the surrounding polymer matrix.

The rigidity of the plasticizers might influence  $\Delta H_{\text{mix}}$  by altering the interaction sites and  $\Delta S_{\text{mix}}$  by altering the polymer chain order around the molecules. This “lipophobic effect” was similarly discussed by Yau et al.<sup>8</sup> to explain the location of the stiff tryptophane at the hydrophilic–hydrophobic interphase of the cell membrane in membrane proteins and peptides. As found by Giunta et al.<sup>9</sup> using molecular dynamics (MD) simulation, the rigidity can determine whether the plasticizer is dispersed in the polymer matrix or forms clusters located at the filler interphase. Thus, higher plasticizer rigidity can lead to a heterogenous distribution in the polymer matrix and increases the dynamic heterogeneity of the compound.<sup>3</sup>

This article investigates the influence of the rigidity of two plasticizers, namely poly-( $\alpha$ -methylstyrene) (AMS) and indene-coumarone (IC), on the glass transition of a silica-filled polybutadiene rubber (BR) compound. The plasticizers differ in rigidity<sup>9</sup> but are similar in aromaticity and glass transition temperature ( $T_g \approx 45^\circ\text{C}$ ). First, the dynamic glass transitions of the pure plasticizers are investigated. Second, the miscibility of the plasticizers in a BR compound is studied. The miscibility is usually determined by analyzing the glass transition or the phase morphology of the compound as a function of the volume fraction of the plasticizer. One common way for the analysis of the glass transition is the conventional differential scanning calorimetry (DSC).<sup>5</sup> For miscible components, a shift in the glass transition temperature ( $T_g$ ) and a broadening of the glass transition step in the thermogram is expected. Here, we additionally use broadband dielectric spectroscopy (BDS) to investigate the frequency dependence of the dynamic glass transition.

The main relaxation peak in BDS is attributed to the cooperative rearrangements of polymer chain segments and called  $\alpha$ -relaxation. This relaxation corresponds to the dynamic glass transition of the polymer.<sup>10</sup> All glass-forming polymers show at least two relaxation processes.<sup>11</sup> The secondary relaxation process is called  $\beta$ -relaxation is often related with the dynamic of the side

groups.<sup>11,12</sup> However, Johari and Goldstein<sup>13</sup> found that the  $\beta$ -relaxation is a generally feature of the vitrification, which merges with the  $\alpha$ -relaxation at a certain temperature and frequency. They claimed that only in special cases the side groups may predominately cause the secondary relaxation.<sup>12,13</sup> For polybutadiene, several investigations show the merging of the  $\alpha$ -relaxation and the  $\beta$ -relaxation, and controversially discuss the molecular processes behind the relaxation phenomena.<sup>11,14–17</sup>

It is well-proven that the miscibility of polymer blends affects the dielectric relaxation processes, and therefore, can be investigated by BDS.<sup>12,18–20</sup> Besides the evaluation of the glass transition temperature, the dielectric spectroscopy gives deeper insights into the influence of the plasticizers onto the different relaxation processes, the  $\alpha$ -relaxation and the  $\beta$ -relaxation of BR, and an interfacial relaxation process caused by IC molecules expected to be situated at the polymer–silica interface. The visualization of both the miscibility behavior and the accumulation of IC at the silica filler surface is performed by transmission electron microscopy (TEM).

## 2 | EXPERIMENTAL

### 2.1 | Materials

The subject of this investigation is a systematic study of vulcanized, silica-filled BR with varying plasticizer content according to the formulation in Table 1. The chemical structures of the plasticizers are shown in Figure 1.

#### 2.1.1 | Mixing and vulcanization

The compounds were mixed in a two-step mixing process with an 80 ml miniature internal mixer. In the first step, all ingredients except the vulcanization system (DPG, CBS, and sulfur) were mixed at around  $150^\circ\text{C}$ . After adding the vulcanization system in the second step, the compound was mixed at a reduced temperature of around  $80^\circ\text{C}$  to avoid premature crosslinking.

Afterward, samples were vulcanized at  $160^\circ\text{C}$  according to  $t_{90}$ , the time for 90% crosslinking, as listed in Table 2.

### 2.2 | Methods

#### 2.2.1 | Standard differential scanning calorimetry

Standard DSC measurements were performed at a scanning rate of 10 K/min between  $-150$  and  $40^\circ\text{C}$  for the

TABLE 1 Compound formulations

Substance	BR-compounds (phr <sup>a</sup> )
BR <sup>b</sup>	100
Silica	60
TESPD <sup>c</sup>	4.3
6PPD <sup>d</sup>	2.0
Wax <sup>e</sup>	2.0
Zinc oxide	2.5
Stearic acid	2.5
DPG <sup>f</sup>	1.0
CBS <sup>g</sup>	2.0
Sulfur	2.0
AMS <sup>h</sup> or IC <sup>i</sup>	0/10/20/30/40/60/80

Abbreviations: AMS, poly-( $\alpha$ -methylstyrene); BR, butadiene rubber; CBS, N-cyclohexylbenzothiazol-2-sulfenamid; DPG, 1,3-Diphenylguanidine; IC, indene-coumarone; PPD, N-(1,3-dimethylbutyl)-N'-phenyl-p-phenylenediamine; TESPD, bis-[3-(triethoxysilyl)-propyl]-disulfid.

<sup>a</sup>Non-SI Unit, parts per hundred rubber (phr).

<sup>b</sup> $M_w = 561$  kg/mol, PDI = 2.64, microstructure: 96.1% *cis*, 0.4% *vinyl*, 3.5% *trans*.

<sup>c</sup>bis-[3-(triethoxysilyl)-propyl]-disulfid.

<sup>d</sup>N-(1,3-dimethylbutyl)-N'-phenyl-p-phenylenediamine.

<sup>e</sup>Mixture of refined hydrocarbons and plastics.

<sup>f</sup>1,3-Diphenylguanidine.

<sup>g</sup>N-cyclohexylbenzothiazol-2-sulfenamid.

<sup>h</sup>Poly-( $\alpha$ -methylstyrene),  $M_w = 1296$  g/mol, PDI = 1.78.

<sup>i</sup>Indene-coumarone (IC),  $M_w = 1092$  g/mol, PDI = 3.07.

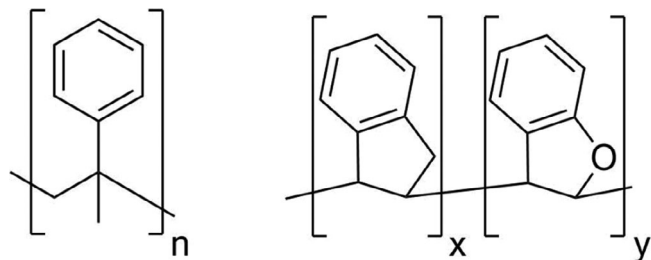


FIGURE 1 Left: Chemical structure of poly-( $\alpha$ -methylstyrene) (AMS). Right: Chemical structure of indene-coumarone (IC). The plasticizers have an average chain length of  $n \approx 10 \approx x + y$ . IC has a proportion of 95% indene and 5% coumarone

rubber compounds and between  $-50$  and  $120^\circ\text{C}$  for the pure plasticizers using a DSC1 (Mettler-Toledo, Greifensee, Switzerland). The annealing time between the scanning runs was 10 min.

## 2.2.2 | Broadband dielectric spectroscopy

The BDS measurements were performed using an Alpha-A High Performance Frequency Analyzer with

TABLE 2 Vulcanization times  $t_{90}$  for the different butadiene rubber compounds

Amount plasticizer (phr)	$t_{90}$ (min)	
	AMS	IC
0	9	
10	9	9
20	9	9
30	11	9
40	11	9
60	12	12
80	14	12

Abbreviations: AMS, poly-( $\alpha$ -methylstyrene); IC, indene-coumarone.

a Novocool cryosystem (Novocontrol Technologies, Montabaur, Germany). Frequency sweeps in the range of  $0.1\text{--}2 \times 10^6$  Hz were performed every five degrees at temperatures between  $-100$  and  $100^\circ\text{C}$  for the rubber compounds and between  $25$  and  $140^\circ\text{C}$  for the pure plasticizer, respectively. The measurements were carried out in a plate capacitor arrangement with a capacitance of  $C = \epsilon \pi D^2 / 4d$  in which the sample has the diameter  $D$ , the thickness  $d$ , and the dielectric permittivity  $\epsilon$ . The complex permittivity  $\epsilon^*(\omega) = C^*(\omega) / C_0$  is calculated for the different angular frequencies  $\omega$  with the capacity of the empty measurement cell  $C_0$ . The rubber samples were prepared as  $d = 0.1\text{--}0.3$  mm and  $D = 30$  mm. The pure plasticizers were molded in a heating press P200S (VOGT Labormaschinen, Berlin, Germany) at  $100^\circ\text{C}$  and  $5.4$  kN for 5 min to a thickness of 0.1 mm.

The modeling of the frequency-dependent permittivity is calculated using the Havriliak–Negami function<sup>21</sup>

$$\epsilon^*(\omega) = \epsilon'(\omega) - i\epsilon''(\omega) = \epsilon_\infty + \frac{\Delta\epsilon}{(1 + (i\omega\tau)^\alpha)^\beta}, \quad (1)$$

where  $\epsilon'(\omega)$  and  $\epsilon''(\omega)$  are the real and imaginary part of the permittivity, respectively,  $i$  is the imaginary unit,  $\epsilon_\infty$  is the high-frequency limit of the real part of the permittivity,  $\Delta\epsilon$  is the relaxation strength,  $\tau$  is the characteristic relaxation time and  $\alpha$ ,  $\beta$  are the shape parameters of the relaxation process. The parameter  $\alpha$  characterizes the slope of the  $\log\epsilon''$  versus  $\log\omega$  peak on the low-frequency side, while the product  $\alpha\beta$  defines the slope on the high-frequency side of the relaxation. If present, the conductivity contribution is considered as  $\sigma(\omega) = -i\sigma_0 / (\epsilon_0\omega)$ , where  $\sigma_0$  is the specific DC conductivity and  $\epsilon_0$  is the vacuum permittivity. For glass-forming systems, the temperature

dependence of the relaxation time  $\tau$  follows the Vogel-Fulcher-Tammann-Hesse equation (VFTH)<sup>22–25</sup>:

$$\log(1/\tau) = A - \frac{B}{T - T_V}, \quad (2)$$

where  $A$  is the logarithm of the pre-exponent factor,  $B$  the curvature parameter and  $T_V$  the Vogel temperature.

### 2.2.3 | Transmission electron microscopy

The TEM investigation was performed on a JEM-1400 (Jeol, Tokyo, Japan) at an acceleration voltage of 100 kV. Samples of 60 nm thin sections were cut with a cryoultramicrotome Leica EM UC6/EM FC6 (Leica Microsystems, Wetzlar, Germany) equipped with a diamond knife at  $-140^\circ\text{C}$ .

## 3 | RESULTS AND DISCUSSION

### 3.1 | Pure plasticizer

Figure 2a shows the dielectric loss spectra of pure AMS and IC. The relaxation peak represents the  $\alpha$ -relaxation related to the dynamic glass transition. The  $\alpha$ -relaxation peak is caused by the frequency-dependent cooperative rearrangement of the polymer chain segments.<sup>26</sup> In case of IC, the  $\alpha$ -relaxation process has a broader distribution of relaxation times as reflected by a broader relaxation peak in Figure 2a. This distribution of relaxation times is expected to be caused by a more heterogenous dynamic of molecular segments.<sup>27</sup> Poly( $\alpha$ -methylstyrene) shows a sharper relaxation peak, and therefore, it is expected to have a more homogenous dynamic of segments. The activation plot in Figure 2b shows the temperature dependence of the relaxation rate,  $\omega_{\max} = 1/\tau_{\max}$ , of the  $\alpha$ -relaxations. The relaxation rate of the DSC measurement at 10 K/min usually corresponds to relaxation times between 100 and 1000 s, which is represented by error bars in the Arrhenius plot.<sup>7,28–31</sup> The determination of the glass transition temperature using DSC is shown in Figure 3. The fit parameters of the VFTH fit are given in Table 3. The curvature parameter  $B$  is related to the fragility index  $m$  defined as  $m = BT_g(T_g - T_V)^{-2}$  where  $T_g$  is conventionally the glass transition temperature for relaxation times of 100 s.<sup>32–34</sup>

As shown in Figure 2b, the temperature dependence of the relaxation times of AMS shows a higher bending compared to IC. Hence, AMS is a more fragile glass

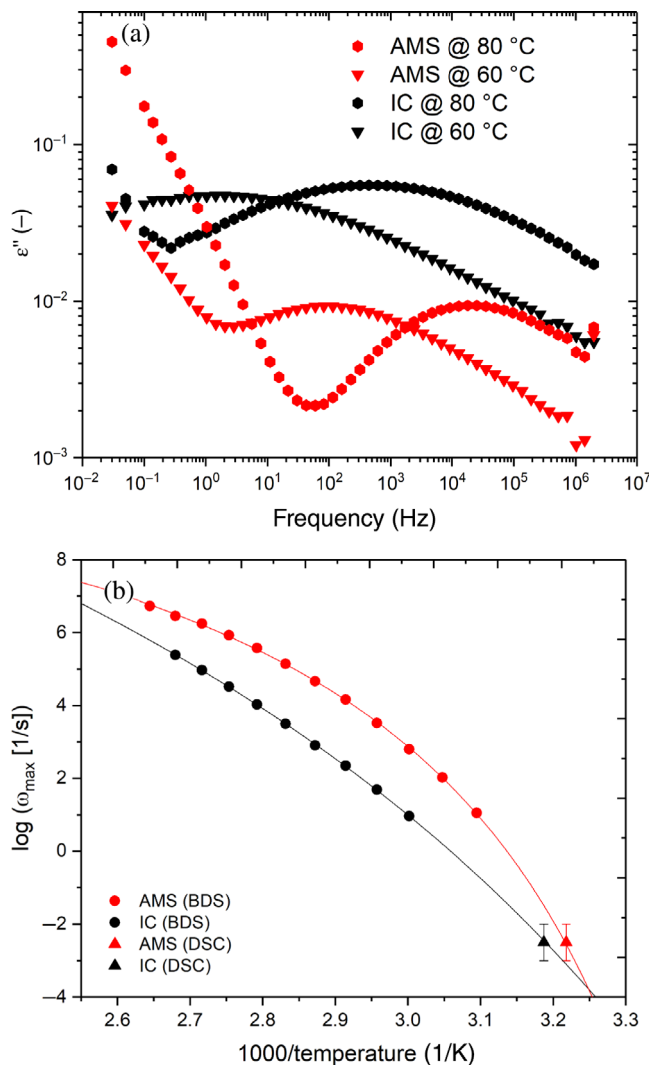


**FIGURE 2** (a) Dielectric loss spectra,  $\epsilon''$  at selected temperatures as function of the frequency for poly-( $\alpha$ -methylstyrene) (AMS) and indene-coumarone (IC), respectively. (b) Temperature dependence of the relaxation rate  $\omega_{\max} = 1/\tau_{\max}$  for AMS and IC measured by broadband dielectric spectroscopy (circles) and differential scanning calorimetry (DSC) (triangles). The error bars for the DSC measurement at 10 K/min consider the variation of relaxation times typically approximated to relaxation times between 100 and 1000 s<sup>7,28–31</sup> [Color figure can be viewed at wileyonlinelibrary.com]

former with a higher fragility index ( $m = 111$ ) compared to the stronger glass former IC ( $m = 64$ ). This finding can be explained with the qualitative concept of the relative flexibility of the side groups and the backbone proposed by Kunal et al.<sup>35</sup> for several polymers. The structure of AMS shows a flexible backbone with bulky side groups leading to a high fragility, while the structure of IC has a rigid backbone with bulky side groups leading to a lower relative flexibility and a lower fragility. These structural

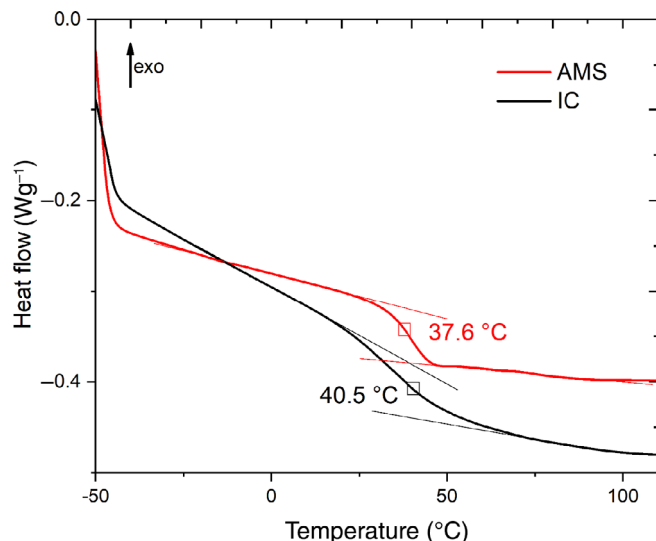


**FIGURE 3** DSC heating curves of AMS and IC measured at 10 K/min. The evaluation of the glass transition temperature is shown. AMS, poly-( $\alpha$ -methylstyrene); IC, indene-coumarone; DSC, differential scanning calorimetry [Color figure can be viewed at [wileyonlinelibrary.com](https://onlinelibrary.com)]

**TABLE 3** Vogel–Fulcher–Tammann–Hesse parameters of fitting Equation (2) and fragility index  $m$  of poly-( $\alpha$ -methylstyrene) (AMS) and indene-coumarone (IC), respectively

Plasticizer	$A$ (–)	$B$ (K)	$T_V$ (K)	$m$ (–)
AMS	12.0	555	272	111
IC	18.6	2107	213	64

differences of the plasticizers are in agreement with the atomistic simulations by Giunta et al.<sup>9</sup> showing a higher flexibility for AMS compared to IC.

### 3.2 | Influence of plasticizers on BR compounds

Figure 4 shows the DSC heating curves for selected compounds. The crystallization peak at around  $-20^\circ\text{C}$  decreases with increasing plasticizer content. At low temperatures, the calorimetric glass transition temperature can be determined in analogy to Figure 3. Figure 5 shows the glass transition temperatures determined by DSC for a non-plasticized BR compound ( $T_g = -102.3^\circ\text{C}$ ) and BR compounds containing different amounts of AMS and IC as plasticizers. As expected from the additive mixing behavior of the substances with different  $T_g$ ,<sup>36</sup> the glass transition temperature increases with increasing plasticizer content, whereat with increasing concentrations, the effect is more pronounced for AMS compared to

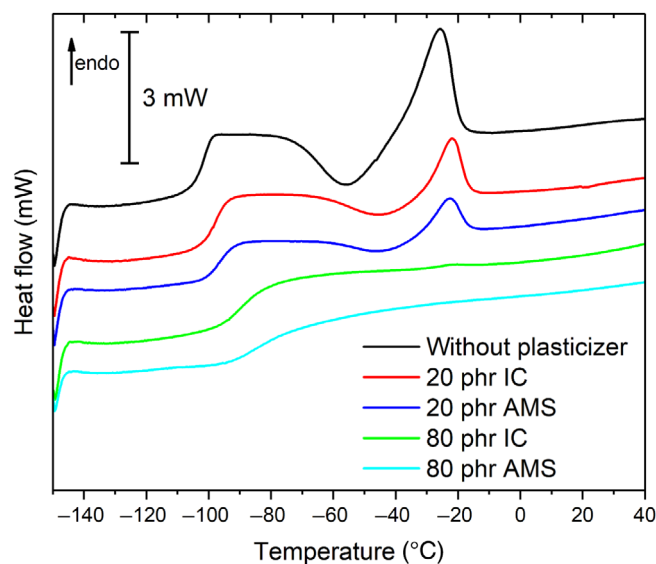


**FIGURE 4** DSC heating curves measured at 10 K/min of the unplasticized compound, the compounds containing 20 and 80 phr AMS and IC, respectively. AMS, poly-( $\alpha$ -methylstyrene); IC, indene-coumarone; DSC, differential scanning calorimetry [Color figure can be viewed at [wileyonlinelibrary.com](https://onlinelibrary.com)]

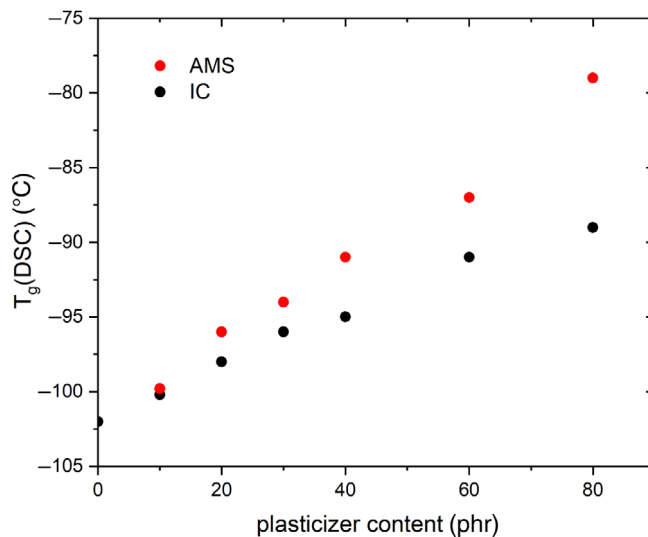


**FIGURE 5** Glass transition temperatures as function of the plasticizer content in butadiene rubber, determined by DSC measurements. Black: IC, red: AMS. AMS, poly-( $\alpha$ -methylstyrene); IC, indene-coumarone; DSC, differential scanning calorimetry [Color figure can be viewed at [wileyonlinelibrary.com](https://onlinelibrary.com)]

IC. The decreased influence on the glass transition temperature of the compound with IC at high concentrations indicates a reduced miscibility of the rigid plasticizer in the polymer matrix.

To gain an insight into the frequency-dependent behavior of the different plasticizer miscibility, BDS measurements of the above-mentioned samples were



performed. The dielectric spectra in Figure 6 show the  $\alpha$ -relaxations of the BR compounds overlapped as a low-frequency shoulder of the corresponding normalized  $\beta$ -relaxations. The  $\alpha$ -relaxations shift with increasing plasticizer content to lower frequencies, as one would expect from the shift in the calorimetric glass transition. The broadening effect of the  $\alpha$ -relaxation increases with increasing content of miscible plasticizer. This is a typical phenomenon assumed to be originating from thermally driven concentration fluctuations.<sup>37–41</sup> In contrast to the shift of the  $\alpha$ -relaxation peak, the  $\beta$ -relaxation appears unaffected in the frequency domain by the variation of the plasticizer. The  $\beta$ -relaxation in polybutadiene is a so-called Johari–Goldstein  $\beta$ -relaxation, which is not independent of the  $\alpha$ -relaxation.<sup>11,15,16</sup> Hence, it is

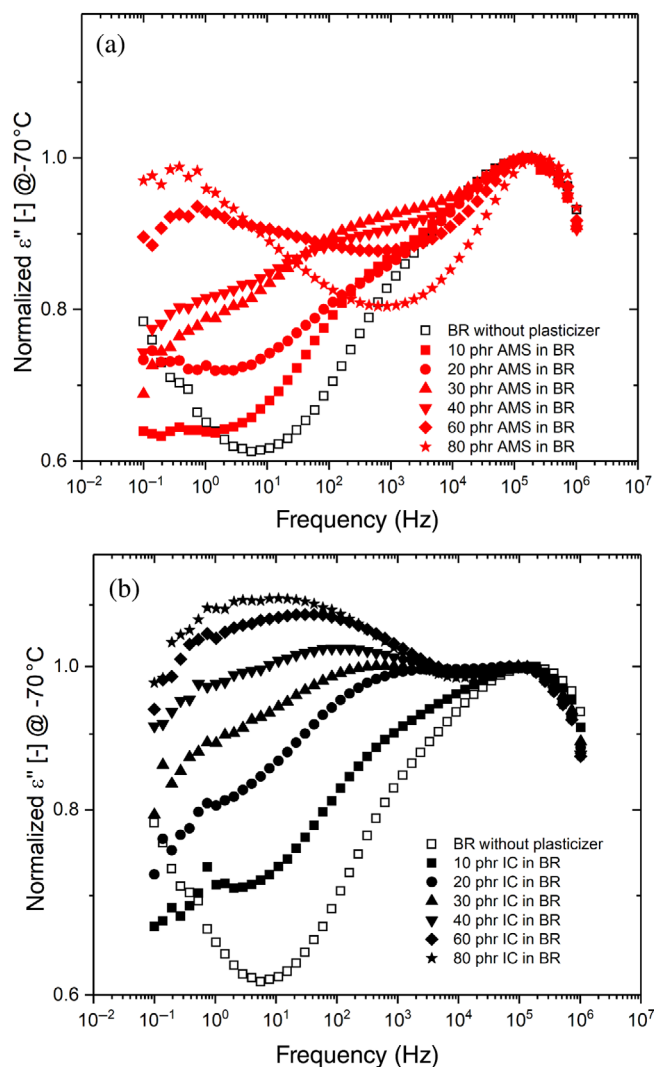


**FIGURE 6** Dielectric loss spectra at  $-70^{\circ}\text{C}$  for the butadiene rubber compounds containing different amounts of AMS (a) and IC (b) normalized to the peak maximum of the  $\beta$ -relaxation. AMS, poly( $\alpha$ -methylstyrene); IC, indene-coumarone [Color figure can be viewed at [wileyonlinelibrary.com](http://wileyonlinelibrary.com)]

noteworthy to mention that the relaxation time of the  $\beta$ -relaxation,  $\tau_{JG}$ , appears to be independent from the  $\alpha$ -relaxation when the relaxation time of the polymer chain segments is shifted by plasticizers. This finding is in agreement with simulation studies of Bedrov and Smith, in which 1,4-polybutadiene was blended with 1,4-polybutadiene with reduced and eliminated dihedral barriers as plasticizer that shows a weak effect of the  $\beta$ -relaxation and a strong shift of the  $\alpha$ -relaxation upon blending.<sup>17</sup>

The relaxation strength of both, the  $\alpha$ -relaxation ( $\Delta\epsilon_{\alpha}$ ) and the  $\beta$ -relaxation ( $\Delta\epsilon_{\beta}$ ), decreases with increasing plasticizer content due to dilution effects. Casalini et al.<sup>42</sup> found a stronger decrease than expected from the composition for  $\Delta\epsilon_{\beta}$  when mineral oil was used as plasticizer and suggested a reduction of the orientability of the polybutadiene. This might explain the relative change of relaxation strength for the compounds plasticized with IC, visible in the normalized dielectric spectra in Figure 6b. This effect seems to be less pronounced if AMS is used as plasticizer, Figure 6a.

A quantitative evaluation of the dielectric spectra would require an unlikely stable fit of the overlapping processes. As discussed by Ngai et al.,<sup>16</sup> the use of empirical fit functions to quantify the overlapping  $\alpha$ -relaxation and  $\beta$ -relaxation in polybutadiene at ambient pressure will lead to misinterpretations of the relaxation time  $\tau_{\beta}$ . Hence, this paper omits the quantitative evaluation and points out the qualitative findings.

Figure 7a shows the dielectric loss at 1 Hz as a function of the temperature normalized to the peak maximum of the  $\alpha$ -relaxation process. The  $\alpha$ -relaxation peaks of BR are visible as one broad process at around  $-95^{\circ}\text{C}$ . The  $\beta$ -relaxations do not arise in the temperature range measured. In both cases, adding plasticizer to the compound again shifts the glass transition to higher temperatures. This shift in temperature for high plasticizer content is more pronounced for AMS than for IC in accordance with the DSC data presented in Figure 5, and it supports the finding of better miscibility of AMS in BR.

The broadening of the  $\alpha$ -relaxation peak is expected to be caused by concentration fluctuations between polybutadiene and the plasticizer as miscible components.<sup>37–39</sup> These concentration fluctuations increase with increasing concentration of the plasticizer in case of miscible blends, while immiscible blends show two separated relaxation peaks with less additional broadening due to less concentration fluctuations.<sup>12,37</sup> Hence, the different broadening of the segmental relaxation can be considered as an additional hint to differences in the miscibility between the polymer and the two plasticizers.

In Figure 7a, the peaks of the  $\alpha$ -relaxation of the two compounds containing a plasticizer amount of 20 phr

each show a comparable width in the dielectric spectra. At a plasticizer content of 80 phr, however, the IC compound shows a narrower  $\alpha$ -relaxation peak compared to the compound plasticized with the more miscible AMS. Thus, less concentration fluctuations are expected to take place in the 80 phr IC compound compared to the 80 phr AMS compound. This reduction in concentration fluctuation might result from a phase separation of IC from polybutadiene, as the fluctuations take place in a small environment next to the polymer chain segments.<sup>39</sup>

The differences in the broadening of the  $\alpha$ -relaxation of the samples containing plasticizers become more obvious at high frequencies (Figure 7b). In the temperature dependence of the dielectric loss at 500 kHz, the sample

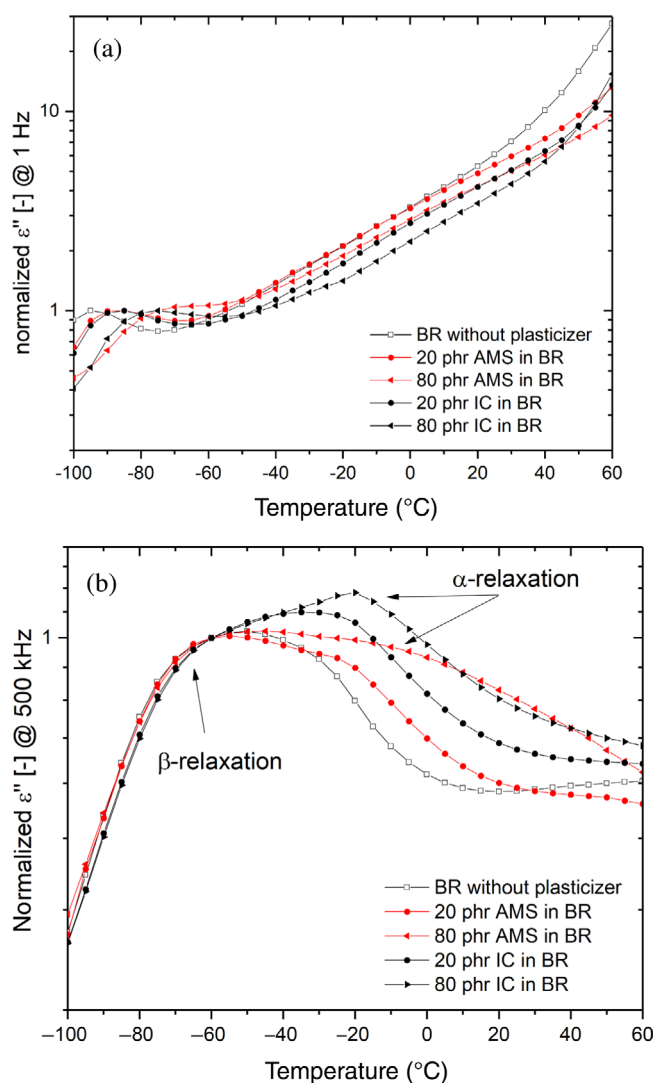


**FIGURE 7** Normalized dielectric loss for selected samples as function of temperature at 1 Hz (a) and 500 kHz (b). The lines are plotted to guide the eye. Dielectric loss is normalized to the maximum of the  $\alpha$ -relaxation (a) and the approximated maximum of the  $\beta$ -relaxation (b) [Color figure can be viewed at [wileyonlinelibrary.com](https://onlinelibrary.wiley.com)]

containing 80 phr IC shows an  $\alpha$ -relaxation peak at  $-20^{\circ}\text{C}$ , while the sample containing 80 phr AMS shows a much broader  $\alpha$ -relaxation at slightly higher temperatures. The high frequency enhances the spatial resolution for processes taking place on small molecular length scales of a few nm.<sup>43–46</sup> Thus, the concentration fluctuation responsible for the broadening of the  $\alpha$ -relaxation predominantly takes place on a small length scale. The strong broadening effect for the sample containing 80 phr AMS leads to the conclusion that the domain sizes of AMS in polybutadiene are smaller compared to the domain sizes of IC in polybutadiene containing the same amount of plasticizer.

This phase separation of IC is also found to be the reason for the deviation of the dielectric loss at high temperatures for BR compounds with and without plasticizers by changing the interfacial properties, for example, at the filler–polymer interface.<sup>9</sup> Figure 8 shows the dielectric loss at  $100^{\circ}\text{C}$  for the pure IC, the BR compound without plasticizer, and the BR compound containing 80 phr AMS and IC, respectively. All dielectric spectra show a strong conductivity contribution at low frequencies. These conductivity contributions are likely due to ionic impurities like water, sodium, or stearic acid. This type of extrinsic conductivity generally increases with a decrease in viscosity according to Stokes' law.<sup>47</sup> The samples show a reduced viscosity at high temperatures, and therefore, the dielectric spectra in Figure 8 show a distinct conductivity contribution. In addition, the compound containing 80 phr IC clearly shows a relaxation

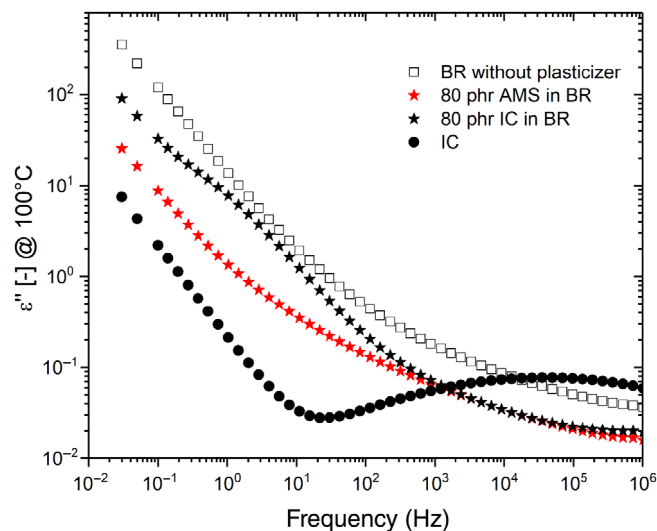


**FIGURE 8** Dielectric loss spectra at  $100^{\circ}\text{C}$  of IC, the BR compounds without plasticizer and containing 80 phr AMS and IC, respectively. AMS, poly-( $\alpha$ -methylstyrene); BR, butadiene rubber; IC, indene-coumarone [Color figure can be viewed at [wileyonlinelibrary.com](https://onlinelibrary.wiley.com)]

peak at around 3 Hz, which is not visible in the other two dielectric spectra. The change in the interfacial relaxation with IC is in accordance with the expectation, that with increasing rigidity of plasticizer, the molecules accumulate at the polymer-filler interphase.<sup>9</sup>

Figure 9 shows the temperature dependence of the relaxation times for the interfacial relaxation process at high temperatures and low frequencies for the compounds with 80 phr IC in comparison to the relaxation processes in pure IC and in the BR compound without plasticizer. The relaxation times were obtained using Equation (1) with  $\beta = 1$  (Cole–Cole equation)

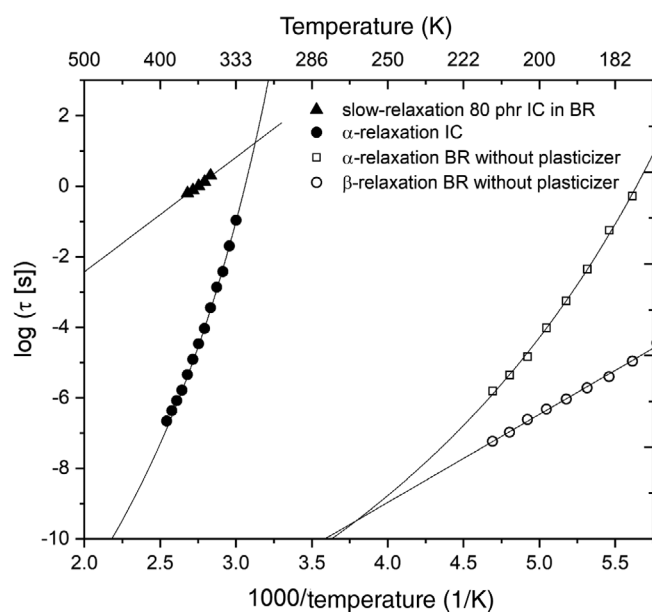


**FIGURE 9** Temperature dependence of the logarithmic relaxation times for IC, the BR compound without plasticizer, and the slow interfacial relaxation in the BR compounds plasticized with 80 phr IC. The solid lines show the VFTH fit for the  $\alpha$ -relaxations or the Arrhenius fit for the  $\beta$ -relaxation and interfacial relaxation, respectively. BR, butadiene rubber; IC, indene-coumarone; VFTH, Vogel–Fulcher–Tammann–Hesse equation

Fit for VFTH behavior	$A$ (–)	$B$ (K)	$T_V$ (K)	$m$ (–)
$\alpha$ -relaxation IC	15.4	1304	243	74
$\alpha$ -relaxation BR without plasticizer	16.7	1094	112	54
Fit for Arrhenius behavior	$A_A$ (–)		$E_a$ (kJ/mol)	
$\beta$ -relaxation BR without plasticizer	19.0		47.8	
Slow, interfacial relaxation 80 phr IC in BR	8.9		62.2	

Note: Above: VFTH parameters obtained by Equation (2), and fragility index  $m$ . Below: Parameters for the Arrhenius behavior obtained by Equation (3).

Abbreviations: BR, butadiene rubber; IC, indene-coumarone; VFTH, Vogel–Fulcher–Tammann–Hesse equation.

superimposed with the above-mentioned conductivity term as fit function. The solid lines show the VFTH fit according to Equation (2) for  $\alpha$ -relaxations. The interfacial process and the  $\beta$ -relaxation follow the Arrhenius equation

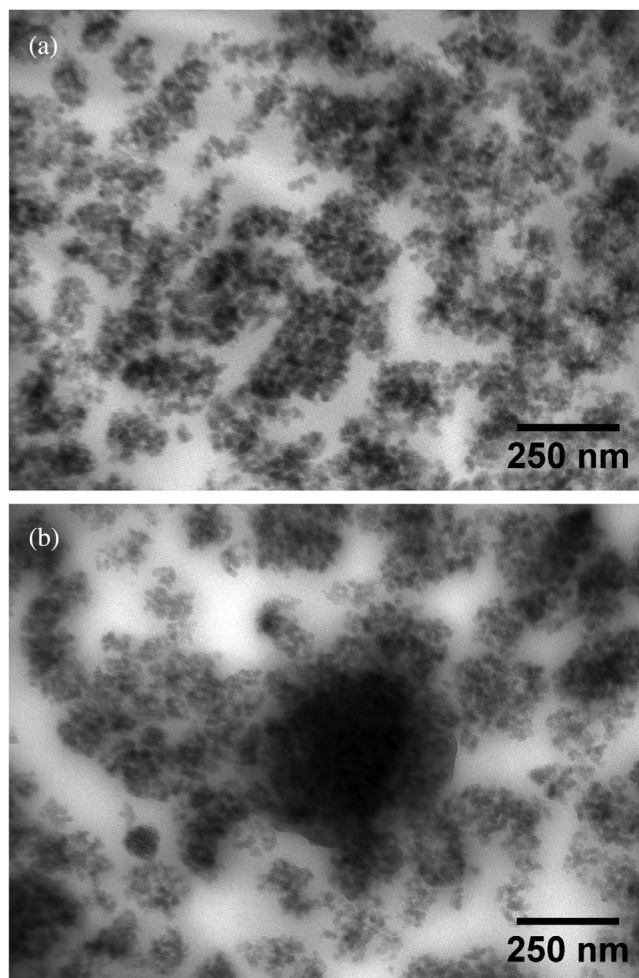


**FIGURE 10** TEM images of the compound with 80 phr AMS in BR (a) and 80 phr IC in BR (b). AMS, poly-( $\alpha$ -methylstyrene); BR, butadiene rubber; TEM, Transmission electron microscopy

**TABLE 4** Parameters for the temperature dependence of the relaxation rate



$$\log(1/\tau) = A_A - \frac{E_a \ln 10}{RT}, \quad (3)$$

where  $A_A$  is the logarithm of the pre-exponent factor,  $E_a$  the apparent activation energy and  $R$  the gas constant. The fit parameters are given in Table 4.

As shown in Figure 9, the interfacial relaxation arising for the compounds containing 80 phr IC exhibit higher relaxation times than the one of pure IC. This indicates that the interfacial relaxation peak at high temperatures is not only affected by the polymer or plasticizer, but also by additional interactions hindering the mobility of the dipoles responsible for this relaxation. As mentioned above, simulation studies show that besides cluster formation, IC molecules tend to be adsorbed at the surface of filler particles.<sup>9</sup> The slow interfacial relaxation at high IC content is likely an interfacial relaxation of IC hindered in mobility due to the adsorption at the silica surface.

The interpretation that the interfacial relaxation is due to adsorbed IC on the silica surface can be experimentally confirmed by TEM imaging. Figure 10a,b show TEM images of the samples with 80 phr AMS and 80 phr IC, respectively. In the case of AMS as plasticizer (Figure 10a), the TEM image shows silica filler particles forming clusters in the polymer matrix. The image showing the sample plasticized with 80 phr IC (Figure 10b) reveals an additional substance, assumed to be IC, surrounding several filler clusters. The IC plasticizer appears to be phase-separated at high concentrations creating domains with a typical size of about 50–100 nm. As shown in Figure 10b, the IC molecules can agglomerate at the silica surface and form larger domains.

## 4 | CONCLUSIONS

The influence of the rigidity of two plasticizers with similar aromaticity, IC and AMS, on their miscibility in a BR compound, and the subsequent shift of the glass transition temperature were investigated using BDS, DSC, and TEM. The results of the BDS investigation of pure plasticizers show a higher fragility for AMS compared to IC in accordance with their relative flexibilities.<sup>35</sup> The shift of the calorimetric glass transition and the relaxation rate of the  $\alpha$ -relaxation confirm that the more rigid IC tends to phase separate at high concentrations. This is in agreement with both TEM imaging and simulation studies<sup>9</sup> showing that IC forms clusters and accumulates at the polymer-filler interphase. The interfacial relaxation of IC at the silica filler surface is slower than the  $\alpha$ -relaxation of the pure plasticizers or of the polymer matrix. Thus, the reduced miscibility of BR and IC at high concentrations of 80 phr is expected to lead to the formation of an

interfacial layer with additional hinderance of the dipoles instead of forming bulk-like phases.

The phase separation becomes more visible in the high-frequency isochronal dielectric spectra due to the different broadening of the  $\alpha$ -relaxations of the two types of plasticizers. Thus, the concentration fluctuation responsible for the broadening of the  $\alpha$ -relaxation in the compound plasticized with AMS is expected to occur at a smaller length scale. In the same way, the domain sizes of AMS in BR are considered to be small compared to those of IC in BR. While the IC domains were visualized by TEM at high concentrations, AMS seems to be dissolved in the BR matrix at a nanometer scale.

The frequency dependence of the  $\beta$ -relaxation seems to be almost unaffected at an IC content of 80 phr in contrast to the BR compound without plasticizer or plasticized with 80 phr AMS. This leads to the conclusion that the rigidity of plasticizers not only affects the miscibility of the plasticizer in BR compounds, but additionally, can change the MDs of the polymer. Since the Johari–Goldstein  $\beta$ -relaxation in BR is not independent of the glass transition, one can conclude that the mechanism of vitrification might change depending on the molecular structure of the plasticizers used.

## ACKNOWLEDGMENT

The authors gratefully acknowledge the permission for publication granted by Continental Tires. Open Access funding enabled and organized by Projekt DEAL.

## AUTHOR CONTRIBUTIONS

**Niclas Lindemann:** Conceptualization (equal); data curation (lead); investigation (lead); methodology (equal); writing – original draft (lead); writing – review and editing (equal). **Sebastian Finger:** Conceptualization (equal); methodology (equal); writing – review and editing (equal). **Hossein Ali Karimi-Varzaneh:** Conceptualization (equal); methodology (equal); writing – review and editing (equal). **Jorge Lacayo-Pineda:** Conceptualization (equal); investigation (equal); methodology (equal); supervision (lead); writing – review and editing (equal).

## DATA AVAILABILITY STATEMENT

The data that support the findings of this study are available from the corresponding author with the permission of Continental Reifen Deutschland GmbH upon reasonable request.

## ORCID

Niclas Lindemann  <https://orcid.org/0000-0002-5247-0093>

Hossein Ali Karimi-Varzaneh  <https://orcid.org/0000-0002-7661-3490>

## REFERENCES

- [1] D. Klat, H. A. Karimi-Varzaneh, J. Lacayo-Pineda, *Polymer* **2018**, *10*, 510.
- [2] S. Datta, in *The Science and Technology of Rubber*, Vol. 4 (Eds: B. Erman, J. E. Mark, C. M. Roland), Elsevier Acad. Press, Amsterdam, The Netherlands **2013**. Chap. 12.
- [3] P. Sharma, S. Roy, H. A. Karimi-Varzaneh, *Macromol. Theory Simul.* **2019**, *28*, 1900003.
- [4] B. Rodgers, W. Waddell, in *The Science and Technology of Rubber*, Vol. 4 (Eds: B. Erman, J. E. Mark, C. M. Roland), Elsevier Acad. Press, Amsterdam, The Netherlands **2013**. Chap. 9.
- [5] L. A. Utracki, in *Polymer Blends Handbook*, Vol. 2 (Eds: L. A. Utracki, C. A. Wilkie), Springer Netherlands, Dordrecht, The Netherlands **2014**. Chap. 2.
- [6] L. A. Utracki, D. J. Walsh, R. A. Weiss, in *Multiphase Polymers: Blends and Ionomers* (Eds: L. A. Utracki, R. A. Weiss), American Chemical Society, Washington, DC **1989**. Chap. 1.
- [7] I. S. Gutzow, J. W. P. Schmelzer, *The Vitreous State: Thermodynamics, Structure, Rheology, and Crystallization*, Springer, Dordrecht, The Netherlands **2013**.
- [8] W. M. Yau, W. C. Wimley, K. Gawrisch, S. H. White, *Biochemistry* **1998**, *37*, 14713.
- [9] G. Giunta, *Doctoral Dissertation*, The University of Manchester **2020**.
- [10] F. Kremer, A. Schönhals, in *Broadband Dielectric Spectroscopy* (Eds: F. Kremer, A. Schönhals), Springer, Berlin, Heidelberg, The Netherlands **2003**. Chap. 4.
- [11] R. Arbe, F. Colmenero, *Phys. Rev. E* **1996**, *54*, 3853.
- [12] A. Schönhals, in *Broadband Dielectric Spectroscopy* (Eds: F. Kremer, A. Schönhals), Springer, Berlin, Heidelberg, The Netherlands **2003**. Chap. 7.
- [13] G. P. Johari, M. Goldstein, *J. Chem. Phys.* **1970**, *53*, 2372.
- [14] A. Hofmann, A. Alegría, J. Colmenero, L. Willner, E. Buscaglia, N. Hadjichristidis, *Macromolecules* **1996**, *29*, 129.
- [15] T. C. Ransom, D. Fragiadakis, C. M. Roland, *Macromolecules* **2018**, *51*, 4694.
- [16] K. L. Ngai, S. Capaccioli, M. Paluch, L. Wang, *Philos. Mag.* **2020**, *100*, 2596.
- [17] D. Bedrov, G. D. Smith, *Macromolecules* **2005**, *38*, 10314.
- [18] H. Yin, A. Schönhals, in *Polymer Blends Handbook*, Vol. 2 (Eds: L. A. Utracki, C. A. Wilkie), Springer Netherlands, Dordrecht, The Netherlands **2014**. Chap. 12.
- [19] A. Zetsche, F. Kremer, W. Jung, H. Schulze, *Polymer* **1990**, *31*, 1883.
- [20] P. A. M. Steeman, J. van Turnhout, in *Broadband Dielectric Spectroscopy* (Eds: F. Kremer, A. Schönhals), Springer, Berlin, Heidelberg, The Netherlands **2003**. Chap. 13.
- [21] S. Havriliak, S. Negami, *J. Polym. Sci., Part C: Polym. Symp.* **1966**, *14*, 99.
- [22] H. Vogel, *Phys. Z.* **1921**, *22*, 645.
- [23] G. S. Fulcher, *J. Am. Ceram. Soc.* **1925**, *8*, 339.
- [24] G. Tammann, W. Hesse, *Z. Anorg. Allg. Chem.* **1926**, *156*, 245.
- [25] J. M. Alberdi, A. Alegría, E. Macho, J. Colmenero, *J. Polym. Sci., Part C: Polym. Lett.* **1986**, *24*, 399.
- [26] F. Kremer, A. Loidl, in *The Scaling of Relaxation Processes* (Eds: F. Kremer, A. Loidl), Springer International Publishing, Cham, Switzerland **2018**. Chap. 1.
- [27] S. K. Kumar, R. H. Colby, S. H. Anastasiadis, G. Fytas, *J. Chem. Phys.* **1996**, *105*, 3777.
- [28] A. Cavagna, *Phys. Rep.* **2009**, *476*, 51.
- [29] G. W. Scherer, *J. Am. Ceram. Soc.* **1984**, *67*, 504.
- [30] P. J. Carroll, G. D. Patterson, S. A. Cullerton, *J. Polym. Sci. Polym. Phys. Ed.* **1983**, *21*, 1889.
- [31] K. Trachenko, C. M. Roland, R. Casalini, *J. Phys. Chem. B* **2008**, *112*, 5111.
- [32] R. Böhmer, K. L. Ngai, C. A. Angell, D. J. Plazek, *J. Chem. Phys.* **1993**, *99*, 4201.
- [33] J. E. K. Schawe, *J. Chem. Phys.* **2014**, *141*, 184905.
- [34] R. Böhmer, C. A. Angell, *Phys. Rev. B Condens. Matter* **1992**, *45*, 10091.
- [35] K. Kunal, C. G. Robertson, S. Pawlus, S. F. Hahn, A. P. Sokolov, *Macromolecules* **2008**, *41*, 7232.
- [36] M. Gordon, J. S. Taylor, *J. Appl. Chem.* **1952**, *2*, 493.
- [37] A. Zetsche, E. W. Fischer, *Acta Polym.* **1994**, *45*, 168.
- [38] G. Katana, E. W. Fischer, T. Hack, V. Abetz, F. Kremer, *Macromolecules* **1995**, *28*, 2714.
- [39] T. Gambino, N. Shafqat, A. Alegría, N. Malicki, S. Dronet, A. Radulescu, K. Nemkowski, A. Arbe, J. Colmenero, *Macromolecules* **2020**, *53*, 7150.
- [40] G. Katana, F. Kremer, E. W. Fischer, R. Plaetschke, *Macromolecules* **1993**, *26*, 3075.
- [41] K. L. Ngai, C. M. Roland, *Macromolecules* **1993**, *26*, 6824.
- [42] R. Casalini, K. L. Ngai, C. G. Robertson, C. M. Roland, *J. Polym. Sci. B Polym. Phys.* **2000**, *38*, 1841.
- [43] A. Rathi, M. Hernández, S. J. Garcia, W. K. Dierkes, J. W. M. Noordermeer, C. Bergmann, J. Trimbach, A. Blume, *J. Polym. Sci. B Polym. Phys.* **2018**, *56*, 842.
- [44] B. B. Sauer, P. Avakian, G. M. Cohen, *Polymer* **1992**, *33*, 2666.
- [45] W. Sengers, M. Wübbenhorst, S. J. Picken, A. D. Gotsis, *Polymer* **2005**, *46*, 6391.
- [46] J. Colmenero, A. Arbe, *Soft Matter* **2007**, *3*, 1474.
- [47] J. Mijović, in *Broadband Dielectric Spectroscopy* (Eds: F. Kremer, A. Schönhals), Springer, Berlin, Heidelberg, The Netherlands **2003**. Chap. 9.

**How to cite this article:** N. Lindemann, S. Finger, H. A. Karimi-Varzaneh, J. Lacayo-Pineda, *J. Appl. Polym. Sci.* **2022**, *139*(21), e52215. <https://doi.org/10.1002/app.52215>